

This is the accepted manuscript made available via CHORUS. The article has been published as:

Substrate-controlled ferromagnetism in iron phthalocyanine films due to one-dimensional iron chains

Thomas Gredig, Corneliu N. Colesniuc, Scott A. Crooker, and Ivan K. Schuller

Phys. Rev. B **86**, 014409 — Published 12 July 2012

DOI: [10.1103/PhysRevB.86.014409](https://doi.org/10.1103/PhysRevB.86.014409)

Substrate controlled Ferromagnetism in Iron Phthalocyanine Films due to One-Dimensional Iron Chains

Thomas Gredig^{1,2,*}, Corneliu N. Colesniuc², Scott A. Crooker³, and Ivan K. Schuller²

¹ *Department of Physics and Astronomy, California State University Long Beach,
1250 Bellflower Blvd., Long Beach, CA 90840, U.S.A.*

² *Department of Physics and Astronomy, University of California San Diego,
9500 Gilman Dr., San Diego, La Jolla, CA 92093, U.S.A. and*

³ *National High Magnetic Field Laboratory, Los Alamos National Laboratory, Los Alamos, NM 87545, U.S.A.*

(Dated: June 15, 2012)

Using magneto-optical Kerr effect, SQUID magnetometry and magnetic circular dichroism spectroscopy, ferromagnetism was found below 4.5K in iron phthalocyanine thin films grown by molecular beam epitaxy. The stacking of the molecules can be controlled via deposition temperature and substrate choice. The molecules self-assemble such that quasi one-dimensional iron chains form. The chains are limited in length by the grain size or film thickness which is manipulated using judicious growth methods. Magnetic hysteresis loops show distinct features in the saturation magnetization and susceptibility that depend on the thin film structure and/or substrate. We find two regimes for the magnetic behavior: below temperatures of ~ 25 K, intra-chain interactions couple the Fe ions and produce non-traditional paramagnetic behavior, while at low temperatures below ~ 4.5 K interactions between the one-dimensional chains produce hysteresis, magnetic order, and slow magnetization dynamics.

PACS numbers: 75.30.-m, 68.55.J-, 81.07.Nb, 87.64.ku

Keywords: low-dimensional magnetism, quasi one-dimensional chains, magnetic circular dichroism, magneto-optical Kerr effect, SQUID, ferromagnetism, phthalocyanine, thin film

I. INTRODUCTION

Conventional magnetic thin films can be prepared using standard deposition methods and their magnetic properties in reduced dimensions have been extensively studied.¹ On the other hand, quasi one-dimensional magnetic structures are more challenging to grow and their ferromagnetic properties are less explored. The metal chains that form in such low-dimensional structures may be configured to interact strongly along the chain direction, but only weakly between chains.²⁻⁴ Such designed magnetic systems often have unique and interesting properties.⁵ Several fabrication methods of quasi one-dimensional magnetic chains exist, but self-organization of magnetic ions embedded in a non-magnetic matrix provides several advantages. The non-magnetic matrix and the magnetic ion can be chemically tuned to specific needs and large samples can be prepared.⁶ One such example includes molecules of the metallo-phthalocyanine family, which are planar molecules with a metal ion core surrounded by organic rings.⁷

Phthalocyanines are planar organic molecules with diverse properties, fundamental to both science and technology. Applications of phthalocyanines include organic field effect transistors, gas sensors,⁸ and solar cells.⁹ Several metallo-phthalocyanine based powders and thin films exhibit low-dimensional magnetism.¹⁰⁻¹⁶ Recently, one-dimensional superexchange between metal ions through nitrogen atoms has been revealed by spin-flip inelastic electron tunneling spectroscopy.¹⁷ Previously, powder iron phthalocyanine (FePc) samples were found to exhibit low-temperature long-range ferromagnetic order.^{18,19} In

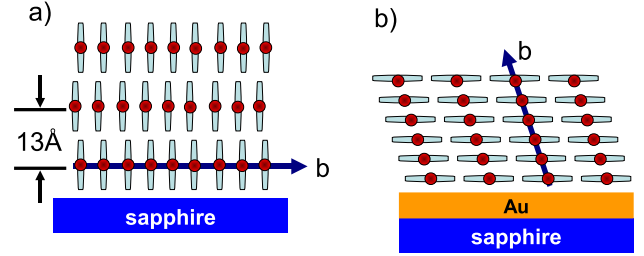


FIG. 1. (Color online) Due to substrate surface - molecule interactions phthalocyanine thin films stack differently on a) sapphire and b) smooth gold surfaces. The arrows point along the crystalline b -axis, which correspond to the direction of the one-dimensional magnetic chains. The circle represents the metal ion and the line represents the organic part of the molecule.

such systems, the iron atoms couple ferromagnetically along quasi one-dimensional chains, while at the same time there is weak antiferromagnetic interaction between chains. Due to weak van-der-Waals forces in organic molecules, several polymorphs of iron phthalocyanine exist. The structural difference of the two most common polymorphs, called the α - and β -phase, is the tilt angle of the molecular stack from the b -axis, which is 26.1° for the α -phase and 44.8° for the β -phase. In FePc powder samples, only the α -phase is ferromagnetic below 10K while the β -phase is known to be paramagnetic down to 1K.²⁰ Remarkably, the opposite holds true for manganese phthalocyanine indicating that the mechanism in iron phthalocyanine is quite different as alluded to earlier.¹⁸ Furthermore, thin films can be deposited with specific sur-

face features as compared to previously studied powder samples.

An important feature of the metallo-phthalocyanine family is the possibility to replace the metal ion and to modify the metal-ion's spacing through the selection of the sample substrate and preparation method, see Fig. 1. Iron phthalocyanine has a divalent Fe^{2+} ion in the center of the molecule that forms quasi one-dimensional (1D) chains when several molecular planes are stacked face to face.²¹ Phthalocyanine powder sublimates near 350°C under high-vacuum and so polycrystalline thin films on heated substrates can easily be deposited.²² In thin films, the directionality of the metal chains is controlled by the growth conditions and through the choice of substrate.²³ As detailed below the metal ion chains can align either perpendicular or parallel to the substrate surface as shown in Fig. 1.

Here, thin films of iron phthalocyanine ($\text{FeC}_{32}\text{N}_8\text{H}_{16}$) are prepared and the magnetic properties are presented for samples grown on different substrates. The substrate influences the stacking type of the molecule and thereby modifies the metal ion inter-distance. As the sample preparation affects the molecular ordering, it can strongly modify the intra-chain distance and therefore the exchange coupling and magnetic interaction. The planar molecules self assemble in the α -phase with a separation of 3.79 \AA along the short monoclinic b -axis.

II. GROWTH

Iron (II) phthalocyanine powder (Sigma-Aldrich) was purified three times using thermal gradient sublimation in vacuum ($< 10^{-6}$ torr).²⁴ Two types of substrates were used for the phthalocyanine deposition to induce different ordering of the molecules.²⁵ The first type is a c -plane sapphire or Si(110) substrate. For the second set, about 40 nm of Au was first deposited by e-beam evaporation onto the substrates. Subsequently, the Au covered samples were annealed in vacuum at 300°C for 1 hour to reduce the surface roughness.²⁶ Additionally, samples were deposited onto cleaned Si(110) substrates, which showed similar growth to that on sapphire substrates based on x-ray diffraction data and atomic force microscopy images.^{21,27}

The FePc was deposited using an effusion cell in an ultra-high vacuum MBE system with a base pressure of $< 5 \times 10^{-10}$ torr. The substrate temperature during the deposition was held near 150°C to increase the order and enhance the crystallinity of the FePc thin films.^{21,27,28} The thickness of FePc was varied from 50 nm to 200 nm and recorded with a quartz crystal monitor. In order to understand the effect of the substrate on the molecular ordering, we prepared sets of samples deposited onto two different substrates. During the FePc sublimation the sapphire and Au-coated sapphire substrates were located side-by-side to ensure identical deposition parameters for both substrates. During the deposition, the substrate

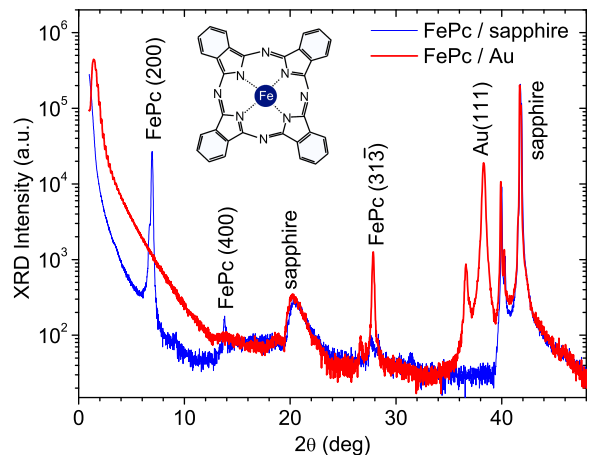


FIG. 2. (Color online) X-ray diffraction spectrum of two co-deposited 60 nm thin FePc films on two different surfaces. The iron phthalocyanine film on sapphire shows prominent (200) and (400) peaks, which are absent from the FePc deposited film on gold. However a prominent 2θ -peak at 28° indicates that the FePc molecule lies flat on the gold surface. The larger background response on gold at low angles ($2\theta < 10^\circ$) is due to the higher electron density of gold as compared to sapphire. The inset shows the chemical structure of iron phthalocyanine.

holder with both samples was rotated to improve the thin film uniformity.

The structure of the organic thin films was characterized with a Rigaku RU-200B x-ray diffractometer using $\text{Cu-K}\alpha$ radiation. Coupled $\theta - 2\theta$ scans, with the momentum transfer vector perpendicular to the substrate plane provides structural information. A superconducting quantum interference device (SQUID) was used to measure magnetization versus temperature curves with the magnetic field applied parallel to the substrate plane. In this case, typical measurement durations for one complete hysteresis loop are about 8 hours. Measurements with the vibrating sample magnetometer (VSM) have been performed at faster rates of 30 to 60 minutes per hysteresis loops. The longitudinal magneto-optical Kerr effect (MOKE) was employed to measure isothermal hysteresis loops in a continuous helium flow cryostat at comparable rates to the VSM measurements.

Magnetic circular dichroism (MCD) spectroscopy spanning the visible spectrum was applied to the FePc films deposited on transparent sapphire or Au-coated sapphire substrates. MCD measures the absorption difference between right- and left-circularly polarized light by the sample in an applied magnetic field. As shown below, MCD provides a clear measure of the out-of-plane magnetization of the FePc film.^{29,30}

III. RESULTS AND ANALYSIS

A. X-ray Diffraction (XRD)

Thin films grown on c-plane sapphire substrates show characteristic first- and second-order peaks, at 6.94° and 13.8° , see Fig. 2. The 6.94° peak corresponds to the (200) peak of the α -phase with lattice spacing of 12.7 \AA indicating that the molecular b -axis is oriented parallel to substrate plane as shown schematically in Fig. 1 a). Additionally, atomic force microscopy images show single molecular steps with a periodicity of 13 \AA that independently confirm this molecular configuration.^{21,27}

Simultaneously grown FePc thin films onto flat Au films with an rms roughness on the order of 7 \AA do not show these low-angle peaks, but instead show a prominent peak at 27.86° .³¹ This peak translates to a Bragg d -spacing of 3.20 \AA . The absence of the low-angle peaks suggests that the molecules order with their planes parallel to the substrate plane so that the b -axis is close to perpendicular to the substrate plane as shown in Fig. 1 b).³²

The different growth modes of phthalocyanine molecules on different substrates provides direct control of the b -axis or the one-dimensional (1D) chain direction in thin films. The competition of molecule-molecule and molecule-substrate interactions generally result in variations of the atomic ordering on the substrate. Since the gold-phthalocyanine interaction is stronger than the phthalocyanine-phthalocyanine interaction, the first layer of phthalocyanine grows flat on the surface.²³ Subsequent layers follow this seed layer. For samples grown on sapphire or silicon substrates, the 1D chains are parallel to the substrate plane, whereas for FePc grown on gold, they are tilted more than 40 degrees with respect to the substrate plane.^{32,33} The average length of the 1D chains can easily be controlled by the substrate deposition temperature for samples grown onto sapphire substrates.²¹ For samples grown onto gold surfaces, the film thickness is proportional to the chain length (up to a maximum thickness equal to the polycrystalline grain size). This creates intriguing options to controllably alter electronic and magnetic properties with growth parameters.

B. Magneto-Optical Kerr Effect (MOKE)

While MOKE is a standard technique to characterize metallic magnetic thin film, it has not been used widely in organic molecular thin films. Recently, Fronk et al. showed that copper and vanadyl phthalocyanine exhibit a significant MOKE signal at room temperature that depends strongly on the molecular orientation.³⁴ Here, we demonstrate that longitudinal MOKE can be applied to measure the magnetic properties of magnetic organic thin films at low temperatures.

MOKE measurements in a parallel field in the temperature range of $8 - 25 \text{ K}$ for gold and sapphire co-deposited thin films are shown in Fig. 3. No hysteretic response is observed in the accessible temperature region of $T > 8 \text{ K}$. However, non-linear behavior with a decreasing saturation intensity indicates non-hysteretic low-field alignment up to about 25 K , see Fig. 3. A comparison between the standing (on Au) and lying (on sapphire) FePc molecular planes shows distinct differences in the slope and shape of the magnetic curves. The magnetic field necessary to saturate the moment for FePc/Au samples is between 800 and 1000 Oe for the temperature range of $8 - 22 \text{ K}$, whereas for the FePc/Si(110) samples, deposited concurrently with the FePc/Au samples, the fields are considerably larger and range from 2000 to 2400 Oe . This is in agreement with SQUID measurements that also show higher susceptibility values ($\partial M / \partial H$) for FePc deposited on gold surfaces. Since each set of samples is deposited simultaneously to guarantee the same growth conditions, we infer that the structural variations produce the different magnetic properties.

C. SQUID Magnetometry

Hysteresis loops have been measured at several temperatures after field-cooling in a 1 T magnetic field. The dc magnetization at 5 K after field-cooling in a 1 T magnetic field shows no coercivity, although the full saturation value of the magnetization is nearly reached. The finite saturation field and lack of hysteretic magnetization are signatures for short-range ordering common to low-dimensional molecular-based ferromagnets. Below 5 K , both FePc on gold and sapphire exhibit hysteretic behavior indicating long-range interaction. At the lowest measured temperature of 2 K the coercivity for FePc of $250 \pm 20 \text{ Oe}$ is observed as shown in Fig. 4.

Even though there is no hysteresis in the intermediate temperature regime between $5 - 25 \text{ K}$, the saturation magnetization decreases only slowly as shown in Fig. 5. The moment at 1 T decreases less than 2% from the 5 K to the 10 K hysteresis loop, which suggests a non-traditional paramagnetic behavior. However at temperatures above 25 K , the saturation magnetization is dramatically reduced. There is qualitative agreement of these measurements with the MOKE data.

D. Magnetic Circular Dichroism (MCD)

Both FePc/sapphire and FePc/Au thin films exhibit strong MCD signals. MCD spectra at different applied perpendicular magnetic fields are shown in Fig. 6. The maximum MCD signal occurs at $\sim 585 \text{ nm}$. Fixing the probe light at this wavelength and sweeping the magnetic field provides a measure of the out-of-plane sample magnetization as a function of field H .

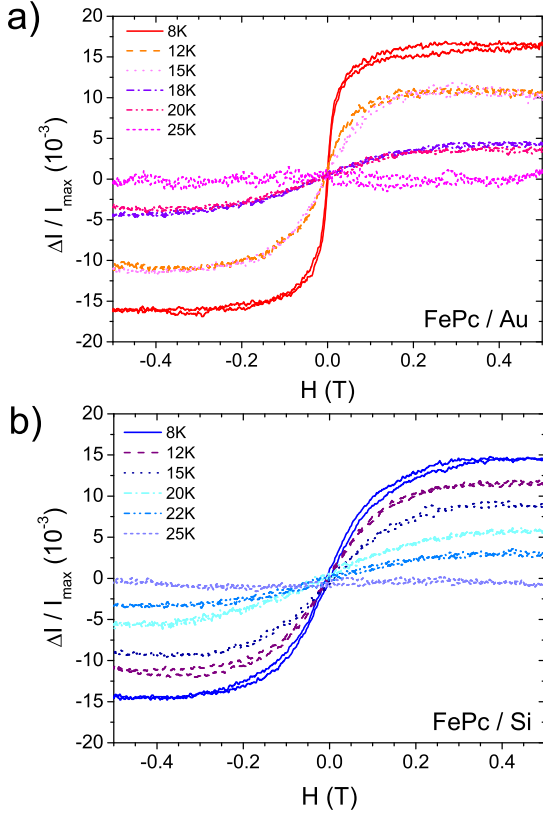


FIG. 3. (Color online) Temperature dependence of longitudinal MOKE magnetization loops for (a) FePc on gold and (b) FePc deposited on a Si(110) surface. The sample is 50 nm thick and deposited at 160°C. No hysteresis is observed above 8K. A linear background is subtracted to illustrate the temperature dependence.

Hysteresis loops at 12 different temperatures are shown in Fig. 7. The coercivity of 400 – 500 Oe at 2K vanishes near 4.5K for the FePc/sapphire samples and near 4K for the FePc/Au samples. These transitions indicate that the onset of long-range magnetic order and hysteresis in these FePc films occurs around a critical temperature of 4.5K. Concomitantly, these MCD measurements also reveal the onset of slow magnetization relaxation dynamics below 4.5K: for example, after ramping the magnetic field to zero from some large initial value, the MCD signals continue to decay on timescales of many minutes (not shown). The width of the hysteresis loops therefore depends on the sweep rate of the magnetic field in the low temperature regime. Above 4.5K, there is no long-range (inter-chain) order or magnetic hysteresis. Rather, there is only non-hysteretic low-field alignment - low field saturation without any hysteresis - that decreases quickly in the temperature range of 10 – 25K.

The inverse of the MCD signal measured at small magnetic fields (effectively, the inverse of the magnetic sus-

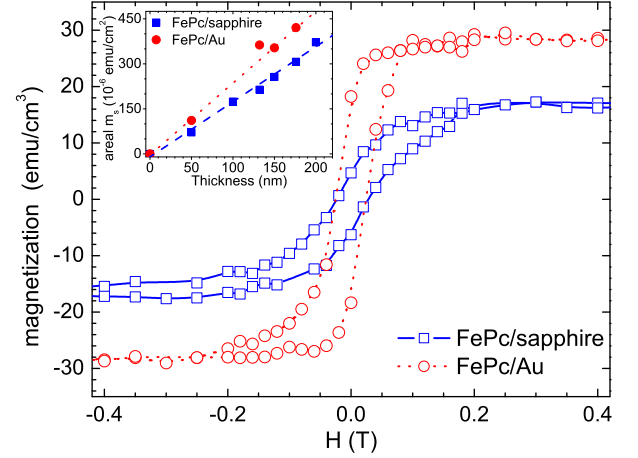


FIG. 4. (Color online) SQUID measurements at 2K show differences in the hysteresis for a sample with 132 nm of iron phthalocyanine deposited on sapphire and gold. The coercivities for both samples are 250 ± 20 Oe, but they have different anisotropy fields and remanent magnetizations. Both samples were deposited side-by-side, and the applied field is in the plane of the thin film. Inset: Thickness dependence of areal saturation moment for a series of FePc samples deposited on sapphire and gold. Lines are linear fits and suggest a higher saturation moment per volume for FePc/Au samples as compared with FePc/sapphire samples.

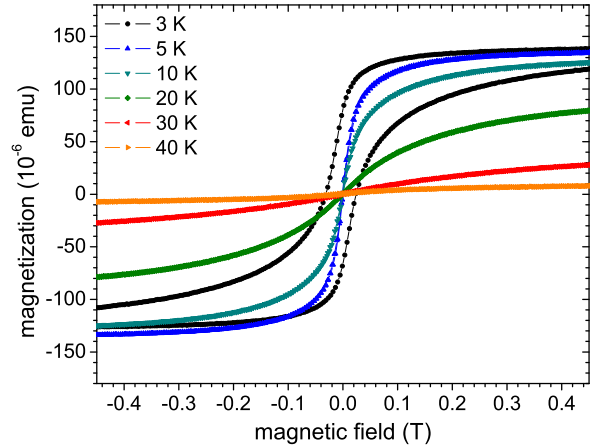


FIG. 5. (Color online) Isothermal hysteresis loops show that hysteretic effects disappear above 4.5K as measured with a vibrating sample magnetometer. Low magnetic fields align the magnetic moments of the iron phthalocyanine film below ~ 25 K. The magnetization is corrected for a diamagnetic background from the substrate.

ceptibility) is plotted in Fig. 8 as a function of temperature for FePc/Au. The data are linear above 60K as expected from a Curie-Weiss law. The positive temperature intercept Θ is 41K, in good agreement with susceptibility measurements on powder α -phase iron phthalocyanine,¹⁸ indicating the onset of coupling between Fe ions within

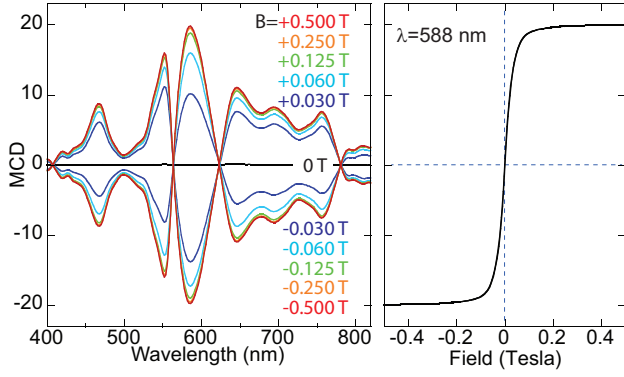


FIG. 6. (Color online) The spectrum of FePc/sapphire as a function of the wavelength exhibits strong MCD response. Each peak in the MCD spectrum corresponds to one of the absorption bands of FePc. The magnetic field curve on the right exemplifies the saturation behavior.

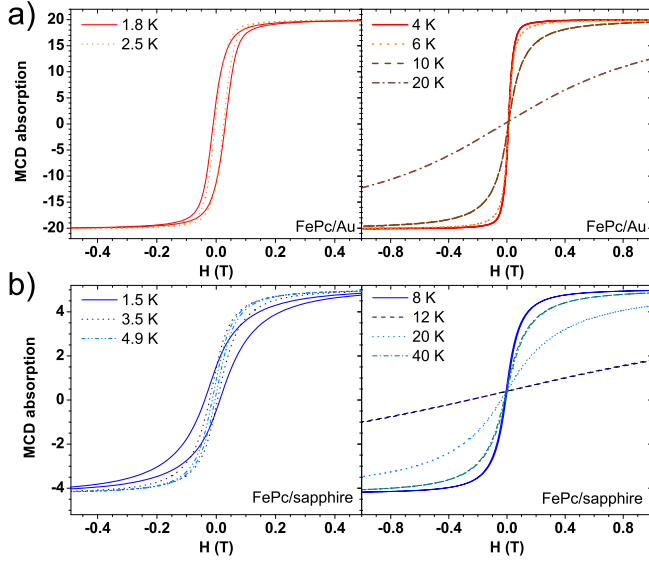


FIG. 7. (Color online) MCD absorption signal as a function of the magnetic field for a) FePc/Au and b) FePc/sapphire thin films. The MCD absorption is measured at $\lambda = 588$ nm and 585 nm for FePc/Au and FePc/sapphire, respectively. The magnetic field is applied perpendicular to the sample plane.

the 1D chains.

E. Analysis

All the data described above indicates that two separate regimes can be qualitatively associated with intra-chain ordering at intermediate temperatures (5 – 25 K) and long-range inter-chain ordering at low temperatures

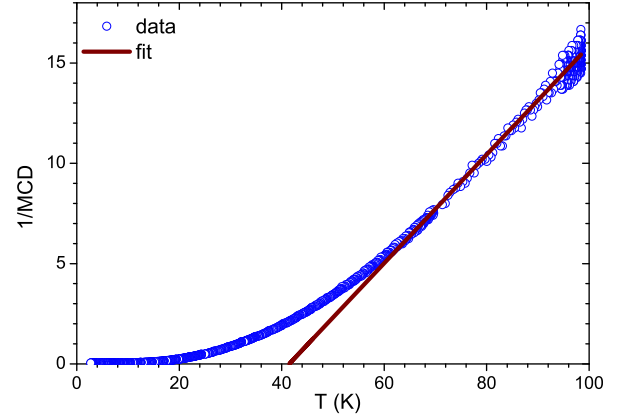


FIG. 8. (Color online) The inverse MCD signal of the FePc/Au sample measured at 0.25 T as a function of temperature is analogous to the inverse susceptibility. The line is a fit to the Curie-Weiss equation with $\Theta = 41$ K.

(below 5 K). Earlier measurements in α -phase FePc powder show that the remanent field increases insignificantly between 25 K and 5 K followed by a much larger increase below 5 K.¹⁸ The long-range inter-chain interaction maybe due to either dipole-dipole interactions³⁵ or weak antiferromagnetic exchange coupling between 1D chains.¹⁸

A representative hysteresis loop in Fig. 4 illustrates the important features in these thin films. The data show fundamental differences in saturation moment, remanence, and zero-field slope with the structure. The saturation magnetization per volume for samples deposited onto gold is larger than co-deposited samples on sapphire. In order to quantify the saturation moment, several FePc samples with different thickness were deposited and the saturation magnetization was measured at 5 K. As shown in the inset of Fig. 4, the magnetic saturation moment scales linearly with thickness as expected. From the slope, the moment is determined to be 18.3 ± 0.7 emu/cm³ for FePc on sapphire, and 23.9 ± 0.4 emu/cm³ for FePc on gold. Using the approximate powder density of 1.6 g/cm³ in combination with the molar mass of FePc, which is 568.4 g/mol, one obtains, $1.2 \mu_B$ and $1.5 \mu_B$ per molecule, respectively. The saturation field - or field strength necessary to saturate the thin film - is generally related to the magnetic anisotropy field. This field is almost twice as large for samples with FePc molecules oriented in the standing configuration on the substrate. In contrast, the anisotropy measured by applying the magnetic field parallel or perpendicular to the substrate, see Fig. 9, shows that the zero-field susceptibilities are similar. However, the magnetization quickly saturates for the FePc thin film with the magnetic field applied perpendicular to the substrate plane. Based on the previous x-ray magnetic circular dichroism measure-

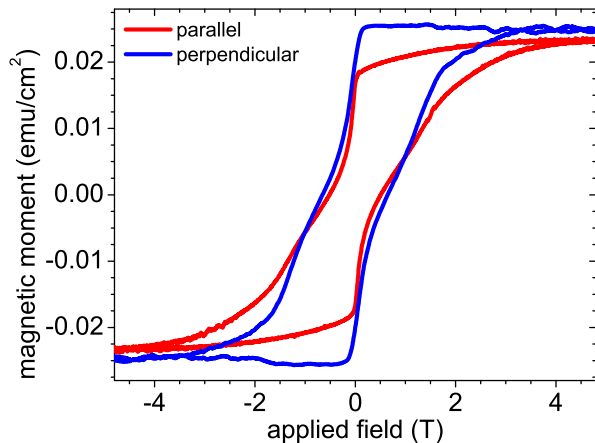


FIG. 9. (Color online) Magnetic anisotropy measured in an FePc/Si sample as measured in a vibrating sample magnetometer at $T=2\text{K}$. The magnetic field is applied either parallel or perpendicular to the plane of the substrate. The slow saturation of the magnetic moment, when the magnetic field is applied parallel to the substrate plane (i.e. the magnetic field is perpendicular to the molecule's plane), supports previous results¹⁶ that the molecule's magnetic moment is slightly tilted away from the molecular plane.

ments, the magnetic moment is neither perpendicular nor parallel to the molecule's plane although closer to the parallel direction.¹⁶ Indeed, the VSM measurements suggest to confirm this property.

Our results show that substrate-induced morphological changes affect both the slope of the magnetization curves as well as the saturation moment. This specific example is an illustration of how magnetic properties in molecular-based organic materials may be tuned via de-

position parameters or the structure.

IV. SUMMARY

Ferromagnetic properties of α -phase iron phthalocyanine thin films were analyzed and compared to previously known properties of α -phase FePc powder samples. Unlike powder FePc for thin films, the structure and the orientation of the Fe chains can be tuned and controlled. Two particularly interesting orientations of FePcs were studied in detail: a) FePc grown on sapphire with the molecular planes orthogonal (i.e. Fe chains parallel) and b) grown on flat gold surfaces with the molecular planes parallel to the substrate (i.e. chains are inclined). MOKE, XMCD and SQUID measurements show the presence of two temperature regimes; above and below $\sim 4.5\text{K}$ resulting from the short-range (paramagnetic) and long-range (ferromagnetic) order due to intra- and inter-iron chain interactions. These results improve the understanding of low-dimensional molecule-based metallo-organic ferromagnets and demonstrate that the hysteresis loop shape, saturation moment, and anisotropy can be controlled using structural manipulation.

ACKNOWLEDGMENTS

This research was supported by the Basic Energy Sciences (BES), U.S. Department of Energy, Grant No. DE-FG03-87ER-45332, the UCOP program on Carbon Nanostructures, and by NSF grant DMR-0847552. One author (T.G.) would like to thank Rafael Morales for his instrumental help with the MOKE alignment and measurement.

* thomas.gredig@csulb.edu

¹ R. Skomski, J. Phys.: Condens. Matter **15**, R841 (2003).

² M. T. Hutchings, E. Samuelsen, G. Shirane, and K. Hirakawa, Phys. Rev. **188**, 919 (1969).

³ M. Steiner, J. Villain, and C. Windsor, Adv. Phys. **25**, 87 (1976).

⁴ C. Dupas and J.-P. Renard, Phys. Rev. B **18**, 401 (1978).

⁵ T. Gredig, P.K. Gentry, C. N. Colesniuc, and I.K. Schuller, J. Mat. Sci. **45**, 5032 (2010).

⁶ D. Gatteschi, Adv. Mat. **6**, 635 (1994).

⁷ G. Liu, T. Gredig, and I.K. Schuller, Europhys. Lett. **83**, 56001 (2008).

⁸ R. D. Yang, T. Gredig, C. N. Colesniuc, J. Park, I.K. Schuller, W. C. Trogler, and A. C. Kummel, Appl. Phys. Lett. **90**, 263506 (2007).

⁹ R. D. Gould, Coord. Chem. Rev. **156**, 237 (1996).

¹⁰ D. Grenoble and H. Drickamer, J. Chem. Phys. **56**, 1017 (1972).

¹¹ A. Labarta, E. Molins, X. Vinas, J. Tejada, A. Caubet, and S. Alvarez, J. Chem. Phys. **80**, 444 (1984).

¹² S. P. Sellers, B. J. Korte, J. P. Fitzgerald, W. M. Reiff, and G. T. Yee, J. Am. Chem. Soc. **120**, 4662 (1998).

¹³ S. Heutz, C. Mitra, W. Wu, A. Fisher, A. Kerridge, M. Stoneham, A. Harker, J. Gardener, H. Tseng, T. Jones, C. Renner, and G. Aeppli, Adv. Mat. **19**, 3618 (2007).

¹⁴ N. Tsukahara, K. I. Noto, M. Ohara, S. Shiraki, N. Takagi, Y. Takata, J. Miyawaki, M. Taguchi, A. Chainani, S. Shin, and M. Kawai, Phys. Rev. Lett. **102**, 167203 (2009).

¹⁵ M. D. Kuz'min, R. Hayn, and V. Oison, Phys. Rev. B **79**, 024413 (2009).

¹⁶ J. Bartolomé, F. Bartolomé, L. M. García, G. Filoti, T. Gredig, C. N. Colesniuc, I.K. Schuller, and J. C. Cezar, Phys. Rev. B **81**, 195405 (2010).

¹⁷ X. Chen, Y.-S. Fu, S.-H. Ji, T. Zhang, P. Cheng, X.-C. Ma, X.-L. Zou, W.-H. Duan, J.-F. Jia, and Q.-K. Xue, Phys. Rev. Lett. **101**, 197208 (2008).

- ¹⁸ M. Evangelisti, J. Bartolomé, L. J. de Jongh, and G. Filoti, *Phys. Rev. B* **66**, 144410 (2002).
- ¹⁹ G. Filoti, M. D. Kuz'min, and J. Bartolomé, *Phys. Rev. B* **74**, 134420 (2006).
- ²⁰ C. G. Barraclough, R. L. Martin, S. Mitra, and R. C. Sherwood, *J. Chem. Phys.* **53**, 1643 (1970).
- ²¹ K. P. Gentry, T. Gredig, and I.K. Schuller, *Phys. Rev. B* **80**, 174118 (2009).
- ²² H. Yamada, T. Shimada, and A. Koma, *J. Chem. Phys.* **108**, 10256 (1998).
- ²³ H. Peisert, T. Schwieger, J. M. Auerhammer, M. Knupfer, M. S. Golden, J. Fink, P. R. Bressler, and M. Mast, *J. Appl. Phys.* **90**, 466 (2001).
- ²⁴ H. J. Wagner, R. O. Loutfy, and C. Hsiao, *J. Mat. Sci.* **17**, 2781 (1982).
- ²⁵ J. R. Ostrick, A. Dodabalapur, L. Torsi, A. J. Lovinger, E. W. Kwock, T. M. Miller, M. Galvin, M. Berggren, and H. E. Katz, *J. Appl. Phys.* **81**, 6804 (1997).
- ²⁶ C. Nogués and M. Wanunu, *Surf. Sci.* **573**, L383 (2004).
- ²⁷ C. W. Miller, A. Sharoni, G. Liu, C. N. Colesniuc, B. Fruhberger, and I.K. Schuller, *Phys. Rev. B* **72**, 104113 (2005).
- ²⁸ Y.-L. Lee, W.-C. Tsai, and J.-R. Maa, *Appl. Surf. Sci.* **173**, 352 (2001).
- ²⁹ P. J. Stephens, *Ann. Rev. Phys. Chem.* **25**, 201 (1974).
- ³⁰ E. I. Solomon, E. G. Pavel, K. E. Loeb, and C. Campochiaro, *Coord. Chem. Rev.* **144**, 369 (1995).
- ³¹ S. Yim, S. Heutz, and T. S. Jones, *Phys. Rev. B* **67**, 165308 (2003).
- ³² I. Biswas, H. Peisert, M. Nagel, M. B. Casu, S. Schuppler, P. Nagel, E. Pellegrin, and T. Chasse, *J. Chem. Phys.* **126**, 174704 (2007).
- ³³ Z. H. Cheng, L. Gao, Z. T. Deng, Q. Liu, N. Jiang, X. Lin, X. B. He, S. X. Du, and H.-J. Gao, *J. Phys. Chem. C* **111**, 2656 (2007).
- ³⁴ M. Fronk, B. Bräuer, J. Kortus, O. G. Schmidt, D. R. T. Zahn, and G. Salvan, *Phys. Rev. B* **79**, 235305 (2009).
- ³⁵ M. A. Girtu, C. M. Wynn, K.-I. Sugiura, J. S. Miller, and A. J. Epstein, *J. Appl. Phys.* **81**, 4410 (1997).